Advanced Composite Materials
Publication details, including instructions for authors and subscription information:
http://www.tandfonline.com/loi/tacm20

Cure monitoring of carbon-epoxy composites by optical fiber-based distributed strain-temperature sensing system

Y. Ito [a] , S. Minakuchi [b] , T. Mizutani [b] & N. Takeda [b]
[a] Department of Aeronautics and Astronautics, Graduate School of Engineering, The University of Tokyo, Tokyo, Japan
[b] Department of Advanced Energy, Graduate School of Frontier Sciences, The University of Tokyo, Tokyo, Japan
Version of record first published: 18 Sep 2012.

To cite this article: Y. Ito , S. Minakuchi , T. Mizutani & N. Takeda (2012): Cure monitoring of carbon-epoxy composites by optical fiber-based distributed strain-temperature sensing system, Advanced Composite Materials, 21:3, 259-271

To link to this article: http://dx.doi.org/10.1080/09243046.2012.723363

Advanced Composite Materials
Vol. 21, No. 3, June 2012, 259–271

Taylor & Francis
Taylor & Francis Group

Cure monitoring of carbon–epoxy composites by optical fiber-based distributed strain–temperature sensing system

Y. Ito[a]*, S. Minakuchi[b], T. Mizutani[b] and N. Takeda[b]

[a]*Department of Aeronautics and Astronautics, Graduate School of Engineering, The University of Tokyo, Tokyo, Japan;* [b]*Department of Advanced Energy, Graduate School of Frontier Sciences, The University of Tokyo, Tokyo, Japan*

(*Received 31 January 2012; final version received 18 June 2012*)

This study establishes an innovative composite cure monitoring technique by utilizing a newly developed hybrid Brillouin–Rayleigh optical fiber sensing system. The new system can separately measure strain and temperature distribution with only one optical fiber. This study began by evaluating the measurement accuracy of the hybrid system in a composite application in a step-by-step manner. A single optical fiber was then embedded in a carbon–epoxy specimen, and thermal residual strain development and temperature change were measured during the cooling period of the curing process. The temperature and residual strain obtained by the hybrid Brillouin–Rayleigh system agreed well with the results measured by a conventional sensor set (i.e. fiber Bragg grating sensors and thermocouples). Furthermore, the system could identify a nonuniform thermal residual strain field induced by a nonuniform cure temperature. These results clearly demonstrated that the proposed technique is quite useful for cure monitoring of large-scale composite structures. Quality assurance for whole parts of actual products can be effectively accomplished by applying the proposed technique.

Keywords: composite; cure monitoring; optical fiber; hybrid Brillouin–Rayleigh system

1. Introduction

Carbon fiber reinforced plastics (CFRPs) have high specific strength and stiffness and have been used extensively in many industrial fields. Their application is rapidly extending to safety-critical primary structures, especially in the field of aircraft. Therefore, quality assurance of large-scale composite structures is necessary, and there is an urgent need to develop effective cure monitoring techniques for composite materials since the quality of the materials is very dependent on their cure processes [1–3]. Several cure monitoring techniques are utilized for composite materials, such as differential scanning calorimetry [4], dielectrometry [5], and point type optical fiber sensors including extrinsic Fabry–Perot type sensors [6,7], Raman spectroscopy [8], and fiber Bragg grating (FBG) sensors [9–11]. Among these techniques, optical fiber sensors are very useful for strain and temperature monitoring of composite materials. Since they are light weight and small, the sensors do not affect the mechanical properties of the materials in which they are embedded. Recently, distributed optical fiber sensors were developed, and these are now considered to be an effective sensing system for structural health monitoring [12–14]. These distributed sensing systems can measure the strain or

*Corresponding author. Email: yusaku@smart.k.u-tokyo.ac.jp

ISSN 0924-3046 print/ISSN 1568-5519 online

http://dx.doi.org/10.1080/09243046.2012.723363
http://www.tandfonline.com

temperature distribution along an optical fiber when the strain or temperature changes. However, since both strain and temperature changes affect the output of the system, they cannot separate the strain and temperature contributions, and thus additional sensors (e.g. thermocouples) are needed for temperature compensation.

A hybrid Brillouin–Rayleigh system [15] was developed to overcome this limitation. This technique utilizes two independent phenomena in an optical fiber, Brillouin and Rayleigh scattering, and can separately measure strain and temperature distribution along the optical fiber. This study develops a new, effective cure monitoring technique by applying this hybrid system to composite materials (Figure 1). First, the strain and temperature coefficients of Brillouin and Rayleigh scatterings are determined by tensile and temperature tests. Simultaneous strain and temperature measurement of a CFRP laminate on which an optical fiber is bonded is performed in tensile tests at different temperatures using the determined coefficients. Finally, an optical fiber is embedded in a CFRP laminate to separately measure the thermal residual strain and temperature change in both uniform and nonuniform temperature fields. The proposed monitoring technique is verified by comparing its results with the results measured by conventional sensors.

2. Measurement principles

The hybrid Brillouin–Rayleigh system consists of a measuring optical fiber, a pulse-prepump Brillouin optical time domain analysis subsystem, and a high-resolution Rayleigh scattering spectrum subsystem. Each subsystem provides measured shifts for Brillouin and Rayleigh scatterings denoted by $\Delta\nu_B$ and $\Delta\nu_R$, when strain and temperature changes are applied. Brillouin scattering is inelastically scattered light with acoustic waves present in the fiber core. The spectrum of the back-scattered light has a peak frequency. The Brillouin frequency shift is determined by measuring the peak frequency shift [16]. In contrast, the spectrum of

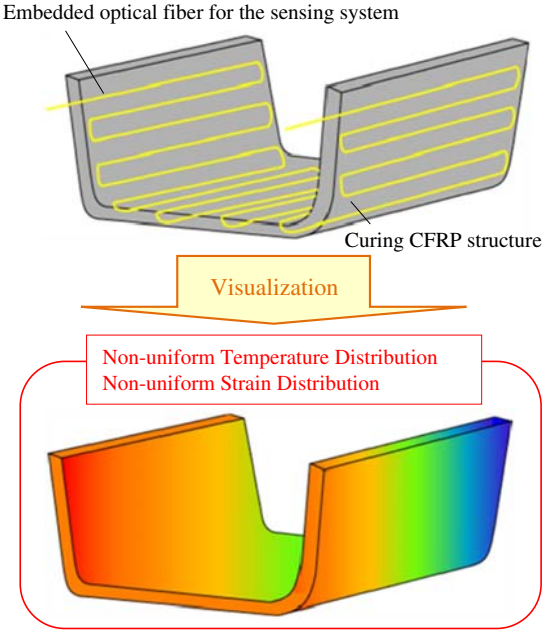

Figure 1. Cure monitoring technique for composite structures using hybrid Brillouin–Rayleigh system.

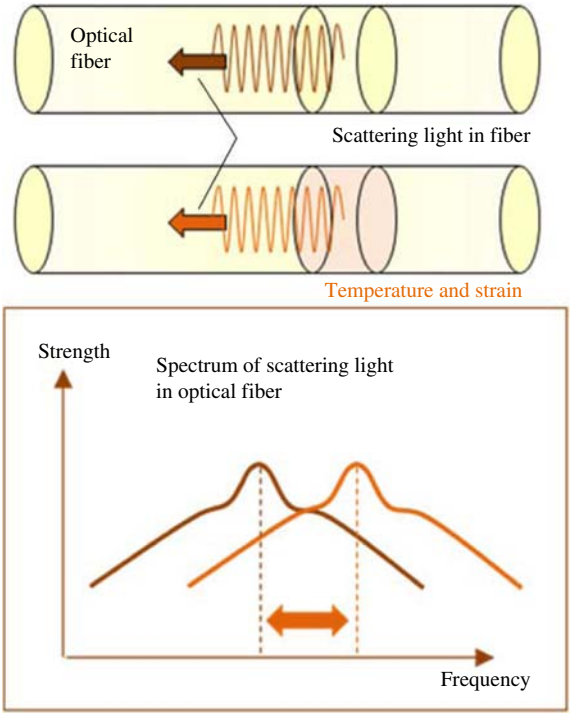

Figure 2. Schematic diagram of frequency shift when the temperature and strain changes.

Rayleigh scattering light has a jagged shape due to interference among a vast number of scattered waves at each scattering source (density distribution and impurities). When the temperature and strain change, the Rayleigh spectrum shifts but retains its shape (Figure 2). The Rayleigh frequency shift is calculated by a cross-correlation analysis between the measurement spectrum and the reference spectrum [17]. The measured shift in the two independent optical scatterings is a function of both applied strain and temperature. Therefore, in the hybrid system, a combination of measured $\Delta\nu_B$ and $\Delta\nu_R$ is used to separate the strain and temperature contributions with the following set of equations:

$$\Delta\nu_B = C_1\Delta\varepsilon + C_2\Delta T \tag{1}$$

$$\Delta\nu_R = D_1\Delta\varepsilon + D_2\Delta T \tag{2}$$

In these equations, $\Delta\varepsilon$ and ΔT are the strain and temperature changes, and C_1 and C_2 are the strain and temperature coefficients for Brillouin scattering. In the same way, D_1 and D_2 are the strain and temperature coefficients for Rayleigh scattering. These coefficients are determined by the experiments described in the next section.

3. Measuring strain and temperature coefficients

3.1. Strain coefficients

The strain coefficients for Brillouin and Rayleigh scattering were measured by tensile tests of a CFRP laminate on which a measuring optical fiber was attached. Figure 3 presents an

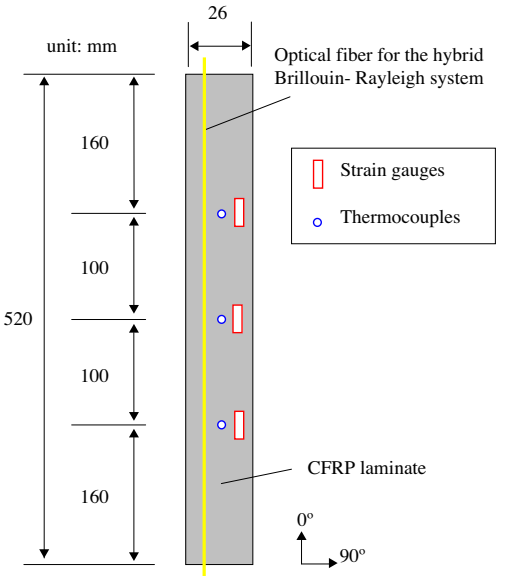

Figure 3. Schematic diagram of specimen and sensors for tensile test.

illustration of a specimen with attached sensors. The measuring optical fiber for the hybrid system, strain gauges, and thermocouples was attached on the specimen surface. The optical fiber was Heatop 300 (polyimide-coated, outer diameter 150 μm, cladding diameter 125 μm), supplied by Totoku Electric Company, Ltd. The material of the specimen was T800S/3900-2B supplied by Toray Industries, Inc. The stacking configuration was $[0_{16}]$. The specimen was cured in an autoclave, and the optical fiber was then bonded on the surface of the specimen by an epoxy adhesive (Araldite AR-R30, Nichiban Company, Ltd). The strain gages (KFG-10-120-C1-11L1M2R, Kyowa Electronic Instruments Co., Ltd) and thermocouples (0.1x1P K-6F, Ninomiya Electric Wire Company, Ltd) were also attached on the same surface. Tensile strains were applied at room temperature and the frequency shifts of both scatterings were measured under each strain condition. The specimen was maintained at a constant temperature (23 °C) during the whole test. Figures 4 and 5 illustrate the relationship between the frequency shift and the applied strain. In both scatterings, the relationships were linear. The strain coefficient

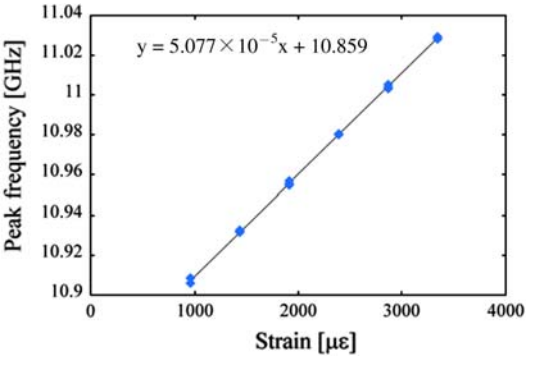

Figure 4. Relation between peak frequency of Brillouin scattering and applied strain.

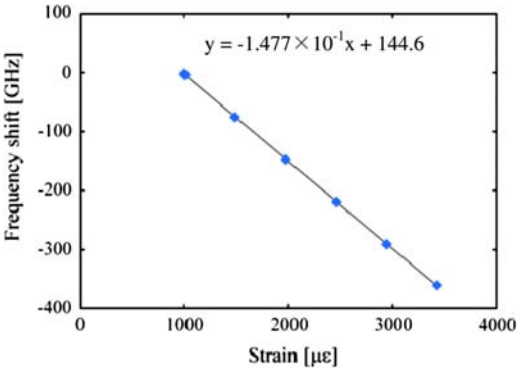

Figure 5. Relation between frequency shift of Rayleigh scattering and applied strain.

of the Brillouin scattering (i.e. the gradients of the graphs) was determined to be $C_1 = 5.077 \times 10^{-5}$ GHz/με and that of Rayleigh scattering, $D_1 = -1.477 \times 10^{-1}$ GHz/με.

3.2. *Temperature coefficients*

The temperature coefficients of the Brillouin and Rayleigh scattering were determined by temperature tests using a thermostatic chamber. A stress-free optical fiber, Heatop 300, was placed in the chamber and the temperature in the chamber was increased step wise from 20 to 200 °C. The frequency shifts were measured at each holding temperature. Figures 6 and 7 illustrate the relationship between the frequency shift and the holding temperature. Again, the relationships were linear. The temperature coefficient of Brillouin scatterings was determined to be $C_2 = 1.090 \times 10^{-3}$ GHz/°C and that of Rayleigh scattering, $D_2 = -1.498$ GHz/°C. All of the determined coefficients are listed in Table 1.

4. Tensile test of composite at different temperatures

4.1. *Experimental*

The separated strain and temperature measurements taken by the hybrid system were verified by tensile tests of a CFRP laminate at different temperatures. The optical fiber and the specimen were the same as described in Section 3.1. First, the frequency shifts of the Brillouin

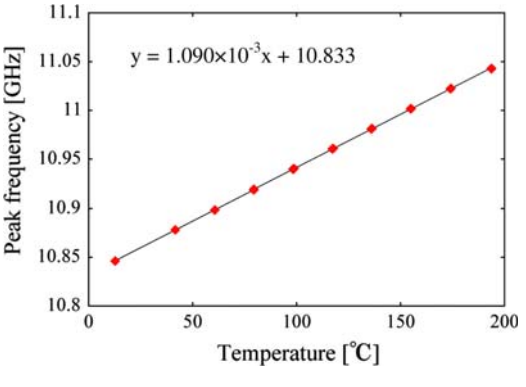

Figure 6. Relation between peak frequency of Brillouin scattering and temperature.

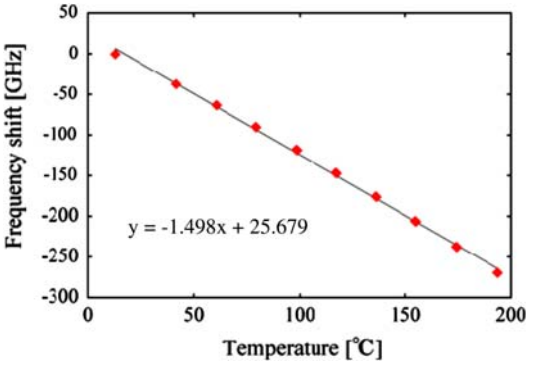

Figure 7. Relation between frequency shift of Rayleigh scattering and temperature.

Table 1. Coefficients in Equations (1) and (2).

Coefficient	Value	Unit
C_1	5.077×10^{-5}	GHz/με
C_2	1.090×10^{-3}	GHz/°C
D_1	-1.477×10^{-1}	GHz/με
D_2	-1.498	GHz/°C

and Rayleigh scatterings were measured at 500, 1000, and 1500 με strain conditions at room temperature (23 °C). The specimen was then unloaded to 0 με and heated to 53 °C by an infrared heater. While the temperature was maintained at a constant value (53 °C), tensile strains were again applied and frequency shifts were measured.

4.2. *Results and discussion*

Figures 8 and 9 illustrate the frequency shifts at the different temperatures. In both scatterings, the contributions of applied strain to the frequency shifts appeared as gradients of the graphs. In contrast, the contributions of temperature change were expressed as gaps in the y axis and were clearly separated from the strain contributions. Using Equations (1) and (2), and the

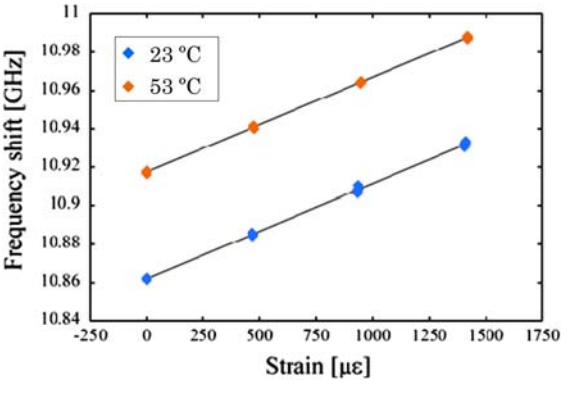

Figure 8. Relation between peak frequency of Brillouin scattering and applied strain.

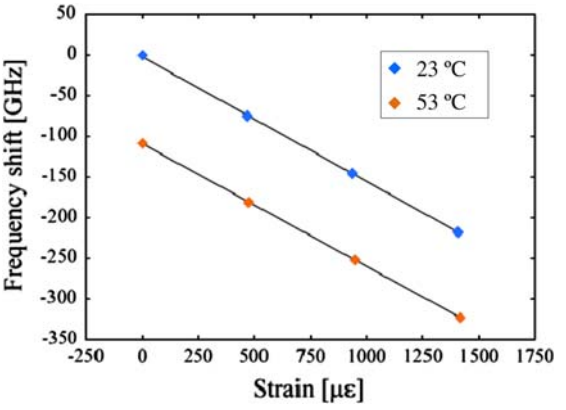

Figure 9. Relation between frequency shift of Rayleigh scattering and applied strain.

Table 2. Calculated temperature changes ΔT and residual strain $\Delta\varepsilon$.

Strain gauges and thermocouples		Hybrid system	
$\Delta\varepsilon$ (με)	ΔT (°C)	$\Delta\varepsilon$ (με)	ΔT (°C)
469	0	520	−3
935	0	974	−2
1408	0	1449	−2
475	31	472	32
948	31	938	32
1419	31	1397	32

coefficients in Table 1, strain and temperature were calculated separately from the measured frequency shifts. Table 2 compares the calculated strain and temperature with the values obtained by the strain gages and the thermocouples. The values obtained from the hybrid system agreed well with those obtained from the conventional sensors. The maximum estimation error was 50 με and 3 °C, and this slight difference may be attributed to the positional difference between the sensors. It was confirmed that the hybrid system can accurately measure the strain and temperature of CFRP laminates with a single optical fiber.

5. Cure monitoring of composite in a uniform temperature field

5.1. Experimental

An optical fiber for the hybrid Brillouin–Rayleigh system was embedded in a CFRP laminate to measure the thermal residual strain and temperature change during the cooling period of the cure process. The optical fiber and material of the specimen were the same as described in previous sections. The stacking configuration was $[90_{16}]$. An FBG sensor and a thermocouple were also embedded for comparison. Figure 10 is an illustration of the specimen indicating the locations of the optical fibers and the thermocouple. All of the sensors were embedded between the eighth and ninth plies. The specimen was cured in an autoclave, with an applied pressure of 0.5 MPa. In this experiment, a uniform temperature field was produced in the specimen using an aluminum plate heater. Figure 11 presents the temperature history during the cure process. As described in Section 2, the Rayleigh frequency shift is calculated

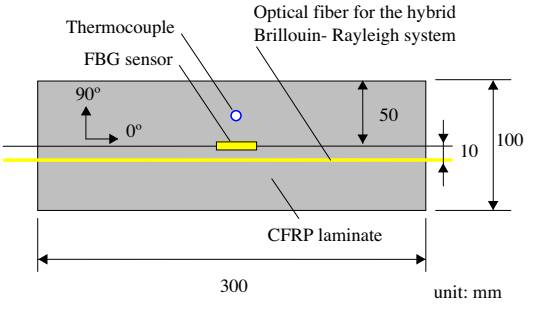

Figure 10. Schematic diagram of specimen with embedded optical fiber sensors and thermocouple.

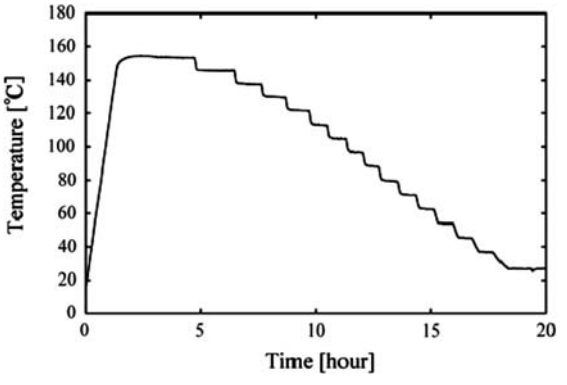

Figure 11. Temperature history measured by thermocouple.

by a cross-correlation analysis between the measurement spectrum and the reference spectrum. When the temperature and strain vary greatly, however, the Rayleigh spectrum shape changes significantly from the reference spectrum and the measurement accuracy decreases. Therefore, in this study, the reference spectrum was updated with each temperature change of 10 °C. In order to maintain the strain and temperature during the measurement, which takes 5 min, a wait time of 20 min was taken at every isothermal holding and the temperature was decreased step-by-step (Figure 11). The total frequency shift of the Rayleigh scattering was calculated by summing these frequency shifts. In contrast, the peak frequencies of Brillouin scattering were measured only at the curing temperature (153 °C) and at the room temperature (27 °C).

5.2. *Results and discussion*

Figures 12 and 13 present the distributions of the Brillouin peak frequencies and a representative Rayleigh frequency shift. In these graphs, the x axis expresses the position of the measuring points along the optical fiber. The portion from 24.4 to 24.7 m corresponds to the embedded area. The distributions of the measured frequency shifts were almost uniform in the specimen. All of the values for the Rayleigh scattering are listed in Table 3. Using these results, the total frequency shifts of the Brillouin scattering were determined to be -3.196×10^{-1} GHz, and that of the Rayleigh scattering to be 713.4 GHz. Substituting these values into Equations (1) and (2), the temperature change and the residual strain were calculated and compared with the values of

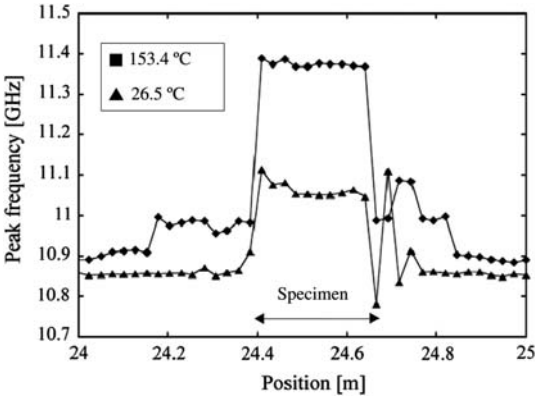

Figure 12. Peak frequencies of Brillouin scattering at 153.4 and 26.5 °C.

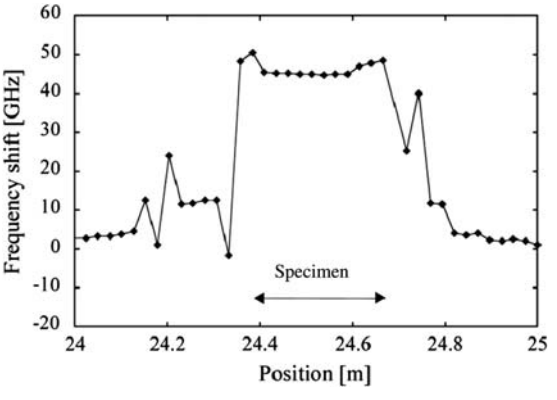

Figure 13. Frequency shift of Rayleigh scattering when temperature changed from 79.5 to 70.9 °C.

Table 3. Frequency shift of Rayleigh scattering $\Delta\nu_R$ at each temperature.

T (°C)	$\Delta\nu_R$ (GHz)	T (°C)	$\Delta\nu_R$ (GHz)
153	–	88	49.0
146	59.6	80	45.3
138	54.3	71	45.2
130	45.2	62	44.8
122	46.5	54	44.5
113	45.4	45	45.5
104	45.0	37	47.7
97	44.7	27	50.8

the FBG sensor and the thermocouple in Table 4. With the hybrid system, the temperature decrease and the compressive strain due to thermal shrinkage could be measured separately, and the values agreed well with those obtained by the FBG sensor and the thermocouple. The difference from the conventional sensors is due to the viscoelastic property of epoxy matrix at high temperatures. Stress relaxation during the measuring time of the proposed technique could decrease the measurement accuracy. Whereas improvements in the measuring speed will be

Table 4. Calculated temperature difference ΔT and residual strain $\Delta\varepsilon$.

	Hybrid system	FBG sensor and thermocouple
ΔT (°C)	−130	−127
$\Delta\varepsilon$ (με)	−3510	−3570

necessary for application to actual structures; these results verify that the proposed technique is able to monitor the thermal residual strain and heat expansion coefficients of cured laminate. The distribution of the degree of cure and the quality of cured composite products can be evaluated using these data.

6. Cure monitoring of composite in nonuniform temperature field

6.1. Experimental

The thermal residual strain and temperature change in a nonuniform temperature field were measured using the hybrid Brillouin–Rayleigh system. Figure 14 depicts the specimen indicating the location of the optical fiber. The optical fiber was embedded between the fourth and fifth plies. The specimen was cured in an autoclave with an applied pressure of 0.5 MPa. A nonuniform temperature field was produced during the curing process by two different heaters. The low-temperature part was heated by the bottom aluminum plate heater; the high-temperature part was heated by both the bottom heater and an additional upper heat blanket. The temperature history in these two parts is plotted in Figure 15. Based on this graph, it is clear that a nonuniform temperature field was produced in the curing specimen. The optical fiber and the specimen material were the same as described in previous sections. The stacking configuration was changed to $[90_8]$. Heat from the upper blanket could easily transfer in the thickness direction. The peak frequencies of Brillouin scattering were measured at the curing temperature and at the room temperature; the frequency shifts of Rayleigh scattering were again measured at each holding temperature, and the total frequency shift was calculated by summing the frequency shifts.

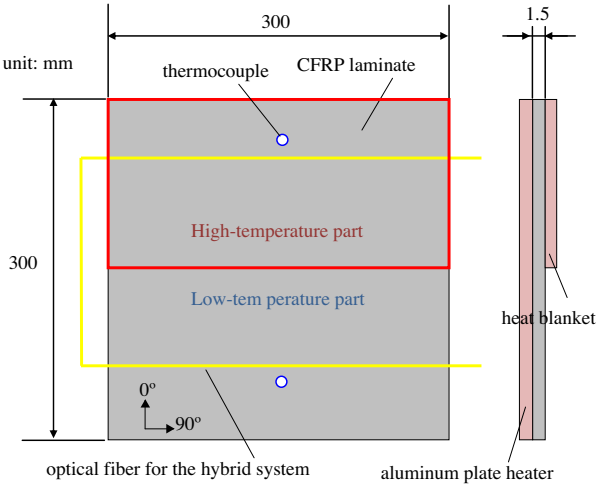

Figure 14. Schematic diagram of specimen with embedded optical fiber sensors and thermocouple.

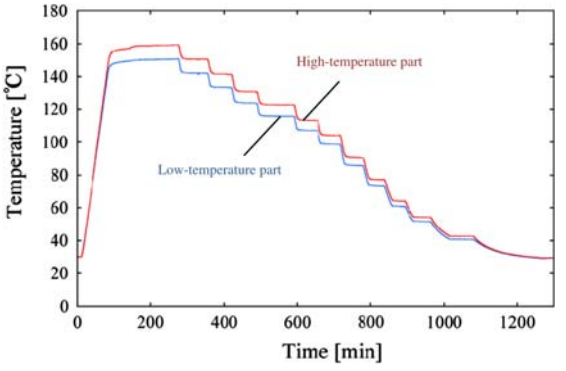

Figure 15. Temperature history measured by thermocouples.

Table 5. Calculated temperature difference ΔT and residual strain $\Delta\varepsilon$.

	High-temperature part	Low-temperature part
ΔT (°C)	−135	−115
$\Delta\varepsilon$ (με)	−4483	−4164

6.2. *Result and discussion*

The temperature change and residual strains were calculated by substituting the measured total frequency shifts of Brillouin and Rayleigh scattering into Equations (1) and (2), (Table 5). In the same laminate, as the temperature gap between curing and room temperatures increased, the residual strain in the cured laminate increased. The differences in temperature and compressive strain caused by the nonuniform temperature field were successfully measured by the hybrid system. These results indicate that the proposed technique would be quite useful for cure monitoring of large-scale composite structures in many industrial fields. Recently, the scale of such structures is becoming larger and their shapes are becoming more complicated due to evolving industrial needs. Thus, it is difficult to keep the whole composite structure at the same temperature during the curing process, and a nonuniform temperature field is inevitable. As seen in the results, the nonuniform temperature field produces a nonuniform residual strain, and this is directly related to the strength of the final products. In this context, the proposed technique enables effective quality assurance for large-scale composite structures by embedding a single optical fiber.

7. Conclusions

This study developed a new, effective cure monitoring technique by applying a hybrid Brillouin–Rayleigh system to composite materials. First, the strain and temperature coefficients of the hybrid system were determined by tensile tests and temperature tests. Using these coefficients, strain and temperature of a CFRP laminate on which an optical fiber was attached were measured by conducting tensile tests at different temperatures. The results of the hybrid system agreed well with other conventional sensors. Next, an optical fiber for the hybrid Brillouin–Rayleigh system was embedded in the CFRP laminate to separately measure the thermal residual strain and temperature change during the cooling

period with uniform and nonuniform temperature fields. Using the hybrid system, the temperature decrease and the compressive strain due to thermal shrinkage could be successfully measured, and the measured values agreed well with those of the conventional sensors. Moreover, the hybrid system successfully measured differences in temperature and compressive strain caused by the nonuniform temperature field. These results verify that the proposed technique would be quite useful for cure monitoring of large-scale composite structures that may have nonuniform strain and temperature distributions. By applying the proposed technique to the actual manufacturing of composite products, quality assurance for large-scale composites can be effectively accomplished by embedding a single optical fiber.

Acknowledgment

The authors acknowledge support from the Ministry of Education, Culture, Sports, Science and Technology of Japan under a Grant-in-Aid for Scientific Research (A) (No. 23246146).

References

[1] Bogetti TA, Gillespie JW Jr. Process induced stress and deformation in thick-section thermoset composite laminates. Journal of Composite Materials. 1992;26(5):627–60.
[2] Wisnom MR, Gigliotti M, Ersoy N, Campbell M, Potter KD. Mechanisms generating residual stresses and distortion during manufacture of polymer-matrix composite structures. Composite: Part A. 2006;37(4):522–9.
[3] Zeng X, Raghavan J. Role of tool-part interaction in process-induced warpage of autoclave-manufactured composite structures. Composite: Part A. 2010;41(9):1174–83.
[4] Lee WI, Loos AC, Springer GS. Heat of reaction, degree of cure, and viscosity of Hercules 3501-6 resin. Journal of Composite Materials. 1982;16(6):510–20.
[5] Bang KG, Kwon JW, Lee DG, Lee JW. Measurement of the degree of cure of glass fiber-epoxy composites using dielectrometry. Journal of Materials Processing Technology. 2001;113 (1):209–14.
[6] Doyle C, Martin A, Liu T, Wu M, Hayes S, Crosby PA, Powell GR, Brooks D, Fernandoy G. In-situ process and condition monitoring of advanced fibre-reinforced composite materials using optical fibre sensors. Smart Materials & Structures. 1998;7(2):145–58.
[7] Leng JS, Asundi A. Real-time cure monitoring of smart composite materials using extrinsic Fabry–Perot interferometer and fiber Bragg grating sensors. Smart Materials & Structures. 2002;11 (2):249–55.
[8] Lyon RE, Chike KE, Angel SM. In-situ cure monitoring of epoxy-resins using fiber optic Raman-spectroscopy. Journal of Applied Polymer Science. 1994;53(13):1805–12.
[9] Loleï K, Ruide O, Véronique M, Pascal H. Investigation of process-induced strains development by fibre Bragg grating sensors in resin transfer moulded composites. Composite: Part A. 2011;42 (3):274–82.
[10] Mulle M, Collombet F, Olivier P, Zitoune R, Huchette C, Laurin F, Grunevald YH. Assessment of cure-residual strains through the thickness of carbon–epoxy laminates using FBGs Part II: technological specimen. Composite: Part A. 2009;40(1):1534–44.
[11] Murukeshan VM, Chan PY, Ong LS, Seah LK. Cure monitoring of smart composites using Fiber Bragg grating based embedded sensors. Sensors and Actuators. 2000;79(2):153–61.
[12] Minakuchi S, Takeda N, Takeda S, Nagao Y, Franceschetti A, Liu X. Life cycle monitoring of large-scale CFRP VARTM structure by fiber-optic-based distributed sensing. Composites Part A: Applied Science and Manufacturing. 2011;42(6):669–76.
[13] Kishida K, Li CH. Pulse pre-pump-BOTDA technology for new generation of distributed strain measuring system. In: Ou J, Li H, Daun Z, editors. Structural health monitoring and intelligent infrastructure. Oxfordshire: Taylor & Francis; 2006. 471–7.
[14] Minardo A, Bernini R, Zeni L, Thevenaz L, Briffod F. A reconstruction technique for long-range stimulated Brillouin scattering distributed fibre-optic sensors experimental results. Measurement Science and Technology. 2005;16(4):900–8.

[15] Kishida K, Nishiguchi K, Li CH, Guzik A. An important milestone of distributed fiber optical sensing technology: separate temperature and strain in single SM fiber. Proceeding of the 14th OECC; 2009 July; Hong Kong, p. 13–17.
[16] Horiguchi T, Shimizu K, Kurashima T, Tateda M, Koyamada Y. Development of a distributed sensing technique using Brillouin scattering. Journal of Lightwave Technology. 1995;13(7):1296–302.
[17] Koyamada Y. New technique for distributed strain measurement in optical fibers with very high sensitivity by making use of Rayleigh backscattering. Technical Report of IEICE, OFT98-23, 1998.